JOURNA S

ORIGINAL ARTICLE



Zeolite-I doped graphitic carbon nitride nanocomposite for the photocatalytic degradation of methylene blue dye

Biswadeepak Satapathy

Department of Chemistry, Prananath Autonomous College, Khordha, Odisha, India

ABSTRACT

This study outlines an innovative process for synthesizing a photocatalyst by anchoring ZIF-8 onto graphitic carbon nitride nanosheets (ZGC), demonstrating superior catalytic efficiency in the photocatalytic degradation of Methylene Blue (MB). The synthesis was conducted using a hydrothermal approach, keeping the zeolite content constant while varying the GC composition. The successful preparation of the materials was verified and characterised through XRD, and FTIR, analyses while the reaction mechanism and degradation kinetics were extensively explored. It was observed from the kinetics plots that the fabricated nanocomposite exhibited significantly enhanced photocatalytic activity for MB degradation. Scavenger tests utilizing different compounds for trapping various radical species helped to determine the dominant reactive species in the degradation process. This work presents zeolite–GC based photocatalytic system with potential for large-scale applications in eliminating harmful pollutants.

KEY WORDS

Zeolite; Graphitic carbon nitride; Photodegradation; Methylene blue

ARTICLE HISTORY

Received 15 July 2025; Revised 04 August 2025; Accepted 12 August 2025

Introduction

Nanomaterials, with their large surface area-to-volume ratio and the predominance of surface atom interactions, have characteristic chemical, physical, magnetic, electrical, and optical properties that differ from bulk materials. Regulated by quantum and nuclear chemistry, nanomaterials are extremely reactive and thus invaluable in a range of uses including UV-protective sunscreens (based on titanium dioxide and zinc oxide nanoparticles), long-lasting car finishes, and sophisticated medical equipment such as oximeters [1]. The transition from research at the lab scale to industrial-scale use highlights the increasing commercial and societal relevance of nanotechnology.

Graphitic carbon nitride (GC), a nanomaterial with a graphitelike framework, is extensively employed across diverse applications due to its remarkable attributes, such as an optimal bandgap, robust chemical stability, biocompatibility, non-toxic nature, and exceptional resistance to thermal and photochemical degradation. When combined with other nanoscale materials, GC manifests unique and enhanced characteristics [2]. Boasting a bandgap of around 2.7 eV, GC efficiently captures visible light, facilitating low-energy photocatalytic processes [3]. This advantageous bandgap stems from nitrogen atoms and sp2hybridized carbon atoms that form π -conjugated networks. The core structural components of GC include triazine and tri-striazine rings [4,5]. There has been much research aimed at improving its photocatalytic activity through the introduction of different dopants, thus extending its applications in real-world contexts. Among nanomaterials, metal-organic frameworks (MOFs), particularly ZIF-L (Zf), have been studied as potential platforms due to their tunable pore, high surface area, and excellent chemical stability. Zf, a metal ion-based and organic linker-based material, possesses efficient electron transfer and metal-to-ligand charge transfer, enhancing its potential as a photocatalyst. Zf, a 2D zinc-2-methylimidazole MOF, is a hydrogen evolution and pollutant degradation photocatalyst due to its high surface area of 300-500 m²/g, microporous structure, and thermal stability of ~400°C. When surface-modified with semiconductors such as TiO2 or GC, charge separation and

visible-light activity are increased, as illustrated in dye degradation and $\mathrm{CO_2}$ reduction studies [6]. Yet, as a pure photocatalyst, ZIF-L's broad bandgap (~4.9 eV) constrains absorption of visible light, and it has problems of quick electron-hole recombination and photocorrosion under long-term irradiation, tending to need composites to work effectively [7]. The high surface area and porosity of zeolites, coupled with the capability of GC to produce reactive oxygen species under visible light, render their composites highly efficient for photocatalytic applications. These materials are superior in adsorbing and degrading organic contaminants, providing a green and cost-effective method of environmental remediation, particularly wastewater treatment.

The combination of Zf with GC structure increases the adsorption of pollutants, and GC's photocatalytic capacity enhances efficient degradation under visible light. This synergy enhances the number of reactive sites, enabling the degradation of organic pollutants and toxic wastes [8]. In contrast to pure zeolites, which are excellent for adsorbing toxic metal ions in soil remediation but have limited photocatalytic activity, ZF/GC's composite (ZGC) integrate adsorption and degradation capacities, thus suitable for cleaning up complicated pollutants such as MB, a globally researched organic dye common in industrial wastewaters.

Despite such developments, the literature indicates key shortcomings in the development and tuning of ZGC composite for photocatalysis. Although separate studies have analyzed the photocatalytic activity of zeolites and GC, with few studies available regarding their synergistic behavior, especially on the optimization of the composition ratio towards optimal activity [9]. In addition, mechanistic aspects in the generation of reactive species and their contribution to pollutant degradation are not well understood. Few reports have explored the kinetics and stability of these composites under different environmental conditions systematically, which has restricted their scalability for large-scale industrial applications. The environmental viability and cost-effectiveness of the synthesis of ZGC composites at large scale have also not been examined comprehensively, which



has restricted their practical realization in wastewater treatment.

The aim of this research is to fill these gaps through the synthesis of a ZGC composite photocatalyst through a hydrothermal method for the effective degradation of Methylene Blue (MB). With the zeolite content kept constant and GC content varied in a systematic way, the composite ZGC was found to possess better photocatalytic activity. Detailed characterization employing X-ray diffraction (XRD), Fourier-transform infrared spectroscopy (FTIR), ensured successful material synthesis. Kinetic studies and scavenger experiments utilizing EDTA-2Na $^{+}$ (for holes), para-Benzoquinone (for $^{\bullet}O_{2}^{-}$), and Isopropyl alcohol (for $^{\bullet}OH$) showed that superoxide radicals (•O2-) were the major reactive species responsible for MB degradation. This research develops the knowledge base of ZGC composite being eco-friendly photocatalysts, providing a promising platform for industrial-scale wastewater remediation and advancing the area of nanotechnology-based environmental remediation

Materials and Methods

Chemicals required

All the chemicals used were of analytical grade. Zn(NO₃)₂.7H₂O, methyl imidazole, EDTA, DMSO, p-Benzoquinone were obtained from NICE chemicals Ltd. The distilled water utilized throughout the experimentation was obtained from the laboratory.

Characterization techniques

The fabricated samples were analyzed through the X-ray diffraction (XRD) and Fourier transform infrared spectroscopy (FTIR) for phase purity and the detection of the functional groups. The XRD equipment was sourced from BRUKER, whereas the FTIR instrument utilized was from Agilent 650.

Fabrication of photocatalyst

For the preparation of GC, 2 g of urea were well mixed in 20 ml of distilled water and filtered and dried. The resulting sample was also kept in muffle furnace for a period of 2.5h at 550 °C [10]. Then the resulting yellow powder was designated as GC and characterized further. For synthesis of Zf, two different beakers with 0.5g of Zn $(NO_3)_2.7H_2O$ and 0.5g pf methyl imidazole were taken individually in 15 mL of H₂O and DMF separately [11]. Both solutions were blended well for a duration of 12h and the produced mixture was left overnight for 15h. The supernatant was spun off and the remaining solution was centrifuged again and again with methanol and water to precipitate out the impurities. The sample was further dried in oven for 24h to get Zf. To prepare the composite ZGC, the same process was repeated. Following the combination of both the solutions in the beaker, 0.5g of the as-prepared GC was incorporated and the remaining steps were executed as mentioned earlier.

Photocatalytic experiments

For photocatalytic experimentation, 0.5g of the precursors and the composite were separately added to 10 ppm of the prepared 150 mL MB solutions in beakers respectively. The beakers were placed in sunlight for a time span of 80 minutes and in every 20 minutes, the 5mL of the solutions were taken out and the absorbance values were measured using UV-is spectrophotometer. For the scavenger tests, four beakers containing 1mM of each of the scavengers EDTA, Sodium

benzoate (BzNa), p-Benzoquinone (BQ) and DMSO were used for quenching the holes, hydroxyl radicals, superoxide radicals and electrons respectively during the photocatalytic experimentation. The subsequent steps taken were identical to those mentioned above.

Results and Discussions

X-ray Diffraction (XRD) is a non-destructive and generalpurpose technique that is crucial for the characterization of crystalline materials in applications such as materials science, chemistry, and engineering. Through the study of X-ray diffraction patterns, XRD uncovers vital information regarding a material's crystal structure, phase content, and preferred crystal orientation. It also delivers structural information like average grain size, crystallinity degree, lattice strain, and evidence of crystal defects like vacancies or dislocations through techniques like the Scherrer equation or Williamson-Hall analysis. XRD also allows accurate lattice parameter measurement and phase quantification using methods such as Rietveld refinement, making it an essential tool in researching nanomaterials, polymers, ceramics, and alloys under different conditions. Figure 1 shows the X-ray diffraction (XRD) patterns of the samples. For the Zf sample, peaks are identified at $2\theta = 7.27^{\circ}$, 10.36° , 12.81° , 14.62° , 16.51° , 18° , 25.1° , and 26.45°, which link to the (110), (200), (211), (220), (310), (222), (332), and (341) planes of the Zf crystal [12, 13]. The characteristic peak for GC is observed at angles of 13.21°, and 27.67°, corresponding to the (100) and (002) planes of GC, respectively [14]. For the binary composite sample ZGC, distinct diffraction peaks are noted at approximately 27.68° corresponding to GC. Apart from the above, the other characteristic peaks at 7.27°, 12.81°, and 14.62° are observed pertaining to the presence of Zf without any trace of Thus, the diffraction patterns of the ZGC impurities. composite sample reveals the characteristic peaks of both Zf and GC. In addition, the XRD patterns of the composites demonstrate that the intensity of the characteristic diffraction peaks of GC rises within ZGC, whereas the intensity of the characterization peaks of Zf declines. The absence of any other peaks implies that the binary composite has been synthesized successfully and is of high purity.

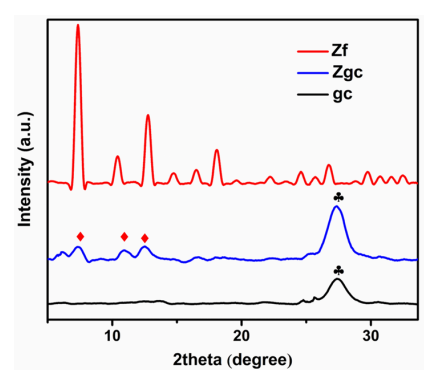


Figure 1. XRD of Zf, GC and binary composite Zf.

Figure 2 illustrates the FTIR spectra for GC, Zf and their composite ZGC. The absorption peaks for GC found in the range of 3000-3500 cm⁻¹, represent the stretching vibrations of N-H and O-H. A range of absorption peaks from 1700-1100 is observed, corresponding to the typical stretching modes of CN heterocycles [15]. Additionally, a sharp absorption peak at 820 cm⁻¹ is attributed to the bending vibrations of triazine units. In case of Zf, peak at 853 cm⁻¹



corresponds to in-plane imidazole ring bending as well as C-C asymmetric stretching [16]. The peaks within the region 1300-1500 cm⁻¹ are associated with the stretching vibrations of the entire imidazole ring, and the peaks within 1500-1585 cm⁻¹ are attributed to C=N stretching bond. The subsequent peaks serve as a crucial characteristic of the ligand structure in Zf. A broad peak within 3200-3600 cm⁻¹ indicates the N-H or O-H stretching vibrations. The nonexistence of a peak at 1850 cm⁻¹ indicates that 2-methylimidazole has been fully deprotonated during the Zf formation, symbolizing its coordination with Zn [17]. The peaks located between 1670-1750 cm⁻¹ may be linked to the unique vibrational modes found in the layered structure or the easy interactions with relatively free 2-methylimidazole ligands. All aforementioned peaks are clearly present in the FTIR spectra of ZGC. However, it could also be observed that the intensity of the absorption peaks becomes more pronounced and broader. This could be assigned owing to the successful intercalation of Zf within GC and their effectual formation.

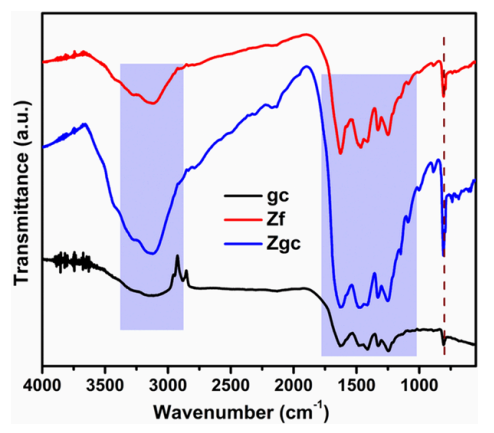


Figure 2. FTIR spectra of Zf, GC and binary composite Zf.

Methylene blue (MB), initially synthesized in 1876 as a textile dye, transitioned into medical use by the late 19th century, starting with malaria treatment and evolving into a key therapy for cyanide poisoning, methemoglobinemia, and ifosfamideinduced neurotoxicity, while also serving as a diagnostic stain and exploring off-label uses like vasoplegic syndrome and neuroprotection [18]. However, its environmental persistence as a non-biodegradable industrial dye has led to its classification as a toxic pollutant, harming aquatic ecosystems and posing health risks like carcinogenicity, and skin irritation, thus necessitating advanced wastewater treatments like photodegradation. Side effects are mild such as blue-green discoloration and nausea, but excessive doses (>5-7 mg/kg) or abuse can lead to serious consequences including hemolysis (particularly in G6PD deficiency), serotonin syndrome, neurotoxicity, paradoxical methemoglobinemia, and cardiovascular complications [19]. Their risks increased by drug interactions and nonpharmaceutical-grade MB, which emphasizes the necessity of medical monitoring [20].

The catalytic efficiency of the precursors GC and Zf along with ZGC were monitored within a span of 80 minutes for the removal of MB. It was observed that the photocatalytic degradation efficiency of the precursors Zf and GC reached 61.2 % and 83.7 % respectively. However, interestingly the photocatalytic efficacy of the binary composite ZGC reached 95.41%. Figure 3a clearly indicates the above findings and presents a graphical overview of change in concentration of MB with time (t). The plot of $-\ln(C/C_0)$ vs time (t) have been plotted

in Figure 3b and the obtained curves have been linearly fitted to get the apparent rate constants. This clarifies that the photodegradation follows pseudo first order kinetics. The histogram as indicated in Figure 3c dictates that the rate constant for the composite is more than the initial components.

There exists a multitude of reactive species that play a role in photocatalytic reactions. These are scrutinized in a reaction through the application of scavengers. Several scavenger tests are carried out to clarify the mechanism of the reaction and to identify the role of the reactive species involved in the reaction [21]. In this investigation, scavenger tests were executed using EDTA (for hole), DMSO (for electrons), BzNa (for OH radical), and BQ (for superoxide radical). It was observed that the degradation percentage dropped to 31.45% and 38.95% in addition of BQ and BzNa indicating that the superoxide radicals are the primary reactive species responsible for photodegradation of MB followed by hydroxyl radicals (Figure 3d). In contrast to this, the degradation percentiles dropped to merely 57.43 % and 61.39 % in case of EDTA and DMSO respectively.

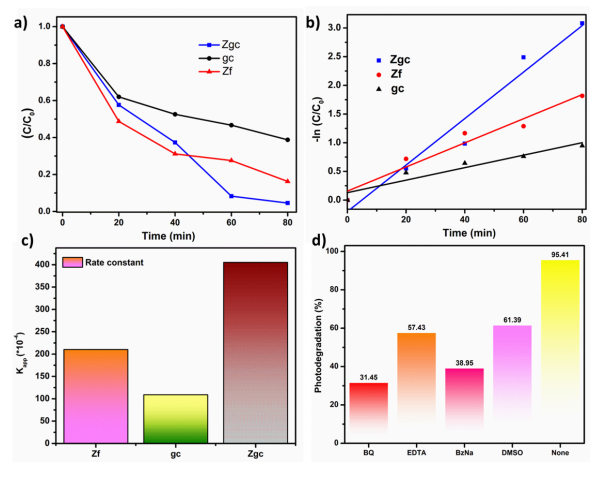


Figure 3. Kinetics plots for photodegradation of MB (a) C/C_0 plot, (b) $-\ln(C/C_0)$ vs t, (c) Apparent rate constants, (d) Scavenger study.

The reusability tests were established to evaluate the stability of the created ZGC photocatalyst. It was found that after three repeated cycles, the degradation rate diminished. This demonstrates that a significant reduction in activity was detected until three consecutive cycles. This validates the stability of the synthesized photocatalyst.

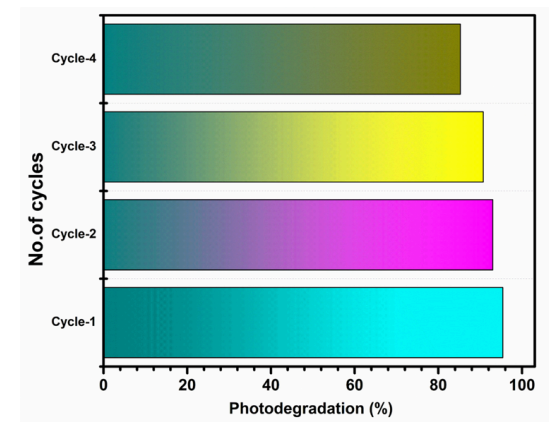


Figure 4. Reusability plot for ZGC.



Conclusions

In summary, this study emphasizes the effective production of a photocatalyst utilizing the solvothermal method. Within a duration of 80 minutes, the resulting binary composite demonstrates a photodegradation rate of 95.41% when exposed to sunlight. The kinetics of the reaction indicate that the degradation process adheres to a pseudo firstorder kinetic model. Additionally, the scavenger analysis reveals that superoxide radicals play a crucial role in the catalyst's effectiveness against the target pollutant MB. The developed photocatalyst exhibits notable recyclability, maintaining an impressive degradation rate of MB even after three successive cycles. This underscores its stability and potential for various other applications.

References

- Smijs TG, Pavel S. Titanium dioxide and zinc oxide nanoparticles in sunscreens: focus on their safety and effectiveness. Nanotechnol Sci Appl. 2011:95-112. https://doi.org/10.2147/NSA.S19419
- Joy J, George E, Vijayan PP, Anas S, Thomas S. An overview of synthesis, morphology, and versatile applications of nanostructured graphitic carbon nitride (g-C3N4). J Ind Eng Chem. 2024;133:74-89. https://doi.org/10.1016/j.jiec.2023.12.016
- Mavengere S, Kim JS. Evaluation of photocatalytic properties of TiO2/g-C3N4 core-shell hybrid catalyst supported on Sr4Al14O25: eu, dy phosphor. J Disper Sci Technol. 2024:1-10. https://doi.org/10.1080/01932691.2024.2378989
- Sahoo S, Acharya R. An overview on recent developments in synthesis and molecular level structure of visible-light responsive g-C3N4 photocatalyst towards environmental remediation. Mater Today Proc. 2021;35:150-155. https://doi.org/10.1016/j.matpr.2020.04.008
- Kumru B, Antonietti M. Colloidal properties of the metalfree semiconductor graphitic carbon nitride. Adv Colloid Interface Sci. 2020;283:102229. https://doi.org/10.1016/j.cis.2020.102229
- Kumar A, Rana S, Sharma G, Dhiman P, Shekh MI, Stadler FJ. Recent advances in zeolitic imidazole frameworks based photocatalysts for organic pollutant degradation and clean energy production. J Environ Chem Eng. 2023;11(5):110770. https://doi.org/10.1016/j.jece.2023.110770
- Wareppam B, Herojit Singh L. ZIFs Recent Development and Its Role in Photocatalysis. InNanostructured Materials and their Applications. 2020:323-336.
- Song J, Zhu L, Yu S, Li G, Wang D. The synergistic effect of adsorption and Fenton oxidation for organic pollutants in water remediation: an overview. RSC Adv. 2024;14(45):33489-33511. https://doi.org/10.1039/D4RA03050H
- Kabadayi O, Altintig E, Ballai G. Zeolite supported zinc oxide nanoparticles composite: Synthesis, characterization, and photocatalytic activity for methylene blue dye degradation. Desalin Water Treat. 2024;319:100433. https://doi.org/10.1016/j.dwt.2024.100433
- Ibrahim A, Memon UB, Kumar JP, Duttagupta SP, Raman RS, Sarkar A, et al. Synthesis, structural and morphological property of a novel Pd/g-CN nano composite for gas sensing application. IOP Conf Ser Mater Sci Eng. 2019;499(1):012003. https://doi.org/10.1088/1757-899X/499/1/012003

- 11. Zhang Y, Jia Y, Li M, Hou LA. Influence of the 2methylimidazole/zinc nitrate hexahydrate molar ratio on the synthesis of zeolitic imidazolate framework-8 crystals at room temperature. Sci Rep. 2018;8(1):9597. https://doi.org/10.1038/s41598-018-28015-7
- 12. Zhong J, Qian L, Wang H, Liu Y, Yao L, Lai Y, et al. Crystalline structure and thermal stability of an unknown ZIF-L300 phase. Inorg Chem. 2023;62(10):4385-4391. https://doi.org/10.1021/acs.inorgchem.3c00160
- 13. Hafner MR, Villanova L, Carraro F. App-based quantification of crystal phases and amorphous content in ZIF biocomposites. Cryst Eng Comm. 2022;24(41):7266-7271. https://doi.org/10.1039/D2CE00073C
- 14. Aparajita P, Das S, Sahoo U, Choudhury S, Pattnayak S, Mallik S, et al. Combinatorial photoactivity enhancement of ternary nanohybrids: Ag cocatalyst-dispersed monoclinic Bi2O3/g-C3N4 through the synergistic action of induced oxygen defect and porosity for abatement of fluoroquinolones and boosted antimicrobial activity. ACS Appl Eng Mater. 2024;2(7):1748-1765. https://doi.org/10.1021/acsaenm.4c00087
- Negro P, Cesano F, Casassa S, Scarano D. Combined DFT-D3 computational and experimental studies on g-C3N4: new insight into structure, optical, and vibrational properties. Mater. 2023;16(10):3644. https://doi.org/10.3390/ma16103644
- 16. Hasegawa K, Ono TA, Noguchi T. Ab initio density functional theory calculations and vibrational analysis of zinc-bound 4methylimidazole as a model of a histidine ligand in metalloenzymes. J Phys Chem A. 2002;106(14):3377-3390. https://doi.org/10.1021/jp012251f
- Edzards J, Saßnick HD, Buzanich AG, Valencia AM, Emmerling F, Beyer S, et al. Effects of ligand substituents on the character of Zn-coordination in zeolitic imidazolate frameworks. J Phys Chem C. 2023;127(43):21456-21464. https://doi.org/10.1021/acs.jpcc.3c06054
- 18. Khan I, Saeed K, Zekker I, Zhang B, Hendi AH, Ahmad A, et al. Review on methylene blue: its properties, uses, toxicity and photodegradation. Water. 2022;14(2):242. https://doi.org/10.3390/w14020242
- Zuschlag ZD, Warren MW, Schultz SK. Serotonin toxicity and urinary analgesics: a case report and systematic literature review of methylene blue-induced serotonin syndrome. Psychosomatics. 2018;59(6):539-546. https://doi.org/10.1016/j.psym.2018.06.012
- 20. Balwani MR, Bawankule CP, Ramteke V, Tolani P, Vakil S, Yadav R. Methylene blue induced methemoglobinemia with acute kidney injury in a glucose-6-phosphate dehydrogenasedeficient patient. Indian J Nephrol. 2017;27(6):465-467. https://doi.org/10.4103/ijn.IJN_316_16
- Vital-Grappin AD, Ariza-Tarazona MC, Luna-Hernandez VM, Villarreal-Chiu JF, Hernandez-Lopez JM, Siligardi C, et al. The role of the reactive species involved in the photocatalytic degradation of HDPE microplastics using C, N-TiO2 powders. Polymers. 2021;13(7):999. https://doi.org/10.3390/polym13070999



11